Ann Rheum Dis 000 (2025) 1–10

Contents lists available at ScienceDirect

Annals of the Rheumatic Diseases

journal homepage: https://www.sciencedirect.com/journal/annals-of-the-rheumatic-diseases

Vasculitis

Exploring the limit of image resolution for human expert classification of vascular ultrasound images in giant cell arteritis and healthy subjects: the GCA-US-AI project

Claus-Juergen Bauer[1,*], Stavros Chrysidis[2], Christian Dejaco[3,4], Matthew J. Koster[5], Minna J. Kohler[6], Sara Monti[7], Wolfgang A. Schmidt[8], Chetan B. Mukhtyar[9], Pantelis Karakostas[1], Marcin Milchert[10], Cristina Ponte[11,12], Christina Duftner[13], Eugenio de Miguel[14], Alojzija Hocevar[15], Annamaria Iagnocco[16], Lene Terslev[17,18], Uffe Møller Døhn[18], Berit Dalsgaard Nielsen[19,20,21], Aaron Juche[22], Luca Seitz[23], Kresten Krarup Keller[19,20], Rositsa Karalilova[24], Thomas Daikeler[25], Sarah Louise Mackie[26,27], Karina Torralba[28], Kornelis S.M. van der Geest[29], Dennis Boumans[30], Philipp Bosch[3], Alessandro Tomelleri[31], Markus Aschwanden[32], Tanaz A. Kermani[33], Andreas Diamantopoulos[34], Ulrich Fredberg[35,36], Nevsun Inanc[37], Simon M. Petzinna[1], Shadi Albarqouni[38,39], Charlotte Behning[40], Valentin Sebastian Schäfer[1]

[1] *Clinic of Internal Medicine III - Rheumatology, University Hospital Bonn, Bonn, Germany*
[2] *Department of Rheumatology, University Hospital of Southern Denmark, Esbjerg, Denmark*
[3] *Department of Rheumatology and Immunology, Medical University Graz, Graz, Austria*
[4] *Department of Rheumatology, Hospital of Bruneck (ASAA-SABES), Teaching Hospital of the Paracelsius Medical University, Bruneck, Italy*
[5] *Division of Rheumatology, Mayo Clinic, Rochester, MN, USA*
[6] *Division of Rheumatology, Allergy and Immunology, Massachusetts General Hospital, Harvard Medical School, Boston, MA, USA*
[7] *IRCCS Istituto Auxologico Italiano, Immunorheumatology Research Laboratory, Milan, Italy*
[8] *Rheumatology, Immanuel Krankenhaus Berlin, Medical Centre for Rheumatology Berlin-Buch, Berlin, Germany*
[9] *Vasculitis Service, Rheumatology Department, Norfolk and Norwich University Hospital, Norwich, UK*
[10] *Department of Rheumatology, Internal Medicine, Geriatrics and Clinical Immunology, Pomeranian Medical University in Szczecin, Szczecin, Poland*
[11] *Department of Rheumatology, ULS de Santa Maria, Centro Académico de Medicina de Lisboa, Lisbon, Portugal*
[12] *Faculdade de Medicina, Universidade de Lisboa, Centro Académico de Medicina de Lisboa, Lisbon, Portugal*
[13] *Department of Internal Medicine, Clinical Division of Internal Medicine II, Medical University Innsbruck, Innsbruck, Austria*
[14] *Department of Rheumatology, Hospital Universitario La Paz, Madrid, Spain*
[15] *Department of Rheumatology, University Medical Centre Ljubljana, Ljubljana, Slovenia*
[16] *Università degli Studi di Torino, Turin, Italy*
[17] *Department of Clinical Medicine, Copenhagen University, Copenhagen, Denmark*

*Correspondence to Dr. Claus-Juergen Bauer.
E-mail address: claus-juergen.bauer@ukbonn.de (C.-J. Bauer).
Handling editor Josef S. Smolen.

https://doi.org/10.1016/j.ard.2025.05.010

[18] Copenhagen Center for Arthritis Research (COPECARE), Center for Rheumatology and Spine Diseases, Rigshospitalet, Glostrup, Denmark
[19] Department of Clinical Medicine, Aarhus University, Aarhus, Denmark
[20] Department of Rheumatology, Aarhus University Hospital, Aarhus, Denmark
[21] Department of Medicine, The Regional Hospital in Horsens, Horsens, Denmark
[22] Department of Rheumatology, Immanuel Hospital, Berlin, Germany
[23] Department of Rheumatology and Immunology, Inselspital, Bern University Hospital, University of Bern, Switzerland
[24] Medical University of Plovdiv, Clinic of Rheumatology, University Hospital "Kaspela", Plovdiv, Bulgaria
[25] Clinic for Rheumatology, University Hospital Basel, Basel, Switzerland
[26] Leeds Institute of Rheumatic and Musculoskeletal Medicine, University of Leeds, Leeds, UK
[27] Leeds Biomedical Research Centre, Leeds Teaching Hospitals NHS Trust, Leeds, UK
[28] Division of Rheumatology, Department of Medicine, Loma Linda University School of Medicine, Loma Linda, CA, USA
[29] Rheumatology and Clinical Immunology, University of Groningen, University Medical Center Groningen, Groningen, The Netherlands
[30] Department of Rheumatology and Clinical Immunology, Hospital Group Twente, Almelo, The Netherlands
[31] Unit of Immunology, Rheumatology, Allergy and Rare Diseases, San Raffaele Scientific Institute, Milan, Italy
[32] Department of Angiology, University Hospital Basel, Basel, Switzerland
[33] Rheumatology, David Geffen School of Medicine, University of California, Los Angeles, CA, USA
[34] Department of Infectious Diseases, Akershus University Hospital, Lørenskog, Norway
[35] Regional Hospital Northern Jutland, Hjorring, Denmark
[36] Department of Rheumatology, Odense University Hospital, Odense, Denmark
[37] Division of Rheumatology, Marmara University School of Medicine, Istanbul, Turkey
[38] Department of Diagnostic and Interventional Radiology, University Hospital Bonn, Bonn, Germany
[39] Helmholtz Munich, Helmholtz AI, Neuherberg, Germany
[40] Institute of Medical Biometry, Informatics and Epidemiology, University Hospital of Bonn, Bonn, Germany

ARTICLE INFO

Article history:
Received 26 December 2024
Received in revised form 10 May 2025
Accepted 12 May 2025

ABSTRACT

Objectives: Prompt diagnosis of giant cell arteritis (GCA) with ultrasound is crucial for preventing severe ocular and other complications, yet expertise in ultrasound performance is scarce. The development of an artificial intelligence (AI)-based assistant that facilitates ultrasound image classification and helps to diagnose GCA early promises to close the existing gap. In the projection of the planned AI, this study investigates the minimum image resolution required for human experts to reliably classify ultrasound images of arteries commonly affected by GCA for the presence or absence of GCA.

Methods: Thirty-one international experts in GCA ultrasonography participated in a web-based exercise. They were asked to classify 10 ultrasound images for each of 5 vascular segments as GCA, normal, or not able to classify. The following segments were assessed: (1) superficial common temporal artery, (2) its frontal and (3) parietal branches (all in transverse view), (4) axillary artery in transverse view, and 5) axillary artery in longitudinal view. Identical images were shown at different resolutions, namely 32 × 32, 64 × 64, 128 × 128, 224 × 224, and 512 × 512 pixels, thereby resulting in a total of 250 images to be classified by every study participant.

Results: Classification performance improved with increasing resolution up to a threshold, plateauing at 224 × 224 pixels. At 224 × 224 pixels, the overall classification sensitivity was 0.767 (95% CI, 0.737-0.796), and specificity was 0.862 (95% CI, 0.831-0.888).

Conclusions: A resolution of 224 × 224 pixels ensures reliable human expert classification and aligns with the input requirements of many common AI-based architectures. Thus, the results of this study substantially guide projected AI development.

INTRODUCTION

Giant cell arteritis (GCA) is the most common form of systemic vasculitis in adults and typically affects large and medium-sized arteries, such as the aorta and temporal and axillary arteries. Signs and symptoms of GCA demand urgent action to verify or exclude a diagnosis in order to prevent severe complications, such as permanent vision loss, which occurs in an average of 20% of all cases [1,2], ischaemic stroke [3–5], and arterial aneurysm and/or dissection [6]. Temporal artery biopsy (TAB) has historically been the diagnostic gold standard but is increasingly being replaced by ultrasound of the temporal and axillary artery as the first-line diagnostic modality in many parts of the world, a practice supported by the latest European Alliance of Associations for Rheumatology (EULAR) recommendations on imaging for GCA [7]. Ultrasound offers widespread use and rapid availability, patient-friendliness, and cost-effectiveness [8], but also excellent image resolution of less than 0.1 mm for superficial arteries with modern ultrasound transducers and the ability to evaluate the entire temporal artery and its branches [9]. This is in contrast to TAB, which may miss GCA detection due to patchy involvement of the artery by vasculitis. The arrival of modern handheld ultrasound devices, characterised by high affordability (<€3000), could further expand future access to point-of-care diagnostic imaging, particularly in resource-limited settings [10]. While their image quality still

WHAT IS ALREADY KNOWN ON THIS TOPIC

- Vascular ultrasound is clinically considered the method of choice for the rapid detection of giant cell arteritis (GCA); however, expertise in ultrasound performance is scarce.
- Artificial intelligence (AI) could assist in image classification, thereby simplifying the examination process.
- However, to develop such an AI, as many AI architectures are constrained by an upper limit of processable image resolution, it is necessary to define the minimum resolution of ultrasound images required to ensure the detection of disease-specific abnormalities.

WHAT THIS STUDY ADDS

- A total of 7750 classification decisions made by 31 international experts were analysed, and 224 × 224 pixels were found to be the minimum image resolution required for the reliable classification of vascular ultrasound images by human experts.
- As this result aligns with the identical critical processing limit for many AI architectures, it allows a wide variety of AI architecture options to be considered for AI development.

HOW THIS STUDY MIGHT AFFECT RESEARCH, PRACTICE OR POLICY

- The findings of this study lay the essential foundation for developing an AI system to assist in ultrasound-based detection of GCA, an approach that holds great potential in allowing rapid diagnosis before ischaemic complications occur and improving examination accessibility even in resource-limited regions.

has some limitations that depend on the specific application, these constraints are expected to decrease with ongoing technological advancements. As a result, these advancements also have the potential to create new educational opportunities for training both specialists and nonspecialists in scanning and interpreting arterial findings in the context of GCA.

GCA ultrasound has proven its excellent reliability [11–16] among experts using appropriate ultrasound equipment, defined as a linear probe ≥7 MHz for axillary artery assessment and a linear probe ≥18 MHz for cranial artery evaluation [17]. However, the examination, especially the interpretation of findings, requires experience and expertise [14,18–20] that are rare to find and mostly limited to specialised centres. While there are initiatives to train rheumatologists all around the globe, these efforts will presumably be insufficient to achieve the desirable goal of a global network of fast-track clinics with sufficient expertise in GCA ultrasound. With modern technological advances, a suggested solution to close this gap is the development of an artificial intelligence (AI)-based assistant (eg, publicly accessible online) that can help classify submitted ultrasound images as abnormal or not, thereby assisting physicians globally in the early detection of GCA.

AI has been proclaimed to lead the fourth industrial revolution and is seen as having the potential to heavily impact our present and future [21]. Likewise, the introduction of AI in the healthcare sector has accelerated quickly over the last few years [22]. Previous attempts to apply AI in the classification of medical image data have proven feasible and have shown remarkable results when trained to label chest radiographs [23], classify skin cancer [24], or identify breast cancer in mammograms [25]. Recently, the first applications of AI in the field of imaging in rheumatology have been made: Andersen et al [26] developed a neural network for the automatic scoring of arthritis disease activity on joint ultrasound images, and Bressem et al [27] trained neural networks for the accurate detection of specific inflammatory joint abnormalities ('sacroiliitis') in pelvic x-rays. However, no attempt has yet been made to utilise AI in GCA for classifying B-mode ultrasound images—standard 2-dimensional greyscale ultrasound images without colour Doppler—as normal or abnormal.

The technological foundation of AI is marked by deep neural networks [28]. A variety of different deep neural network architectures exist, each with distinct characteristics, including limitations in image processing size, resolution, result accuracy, and resource efficiency [28]. In pursuing the outlined development of an AI-based system (see Supplementary Material), it is crucial to consider the technological constraints of diverse neural network architectures. Neural network architectures that are not able to handle images presented in a sufficiently high resolution, necessary for the adequate evaluation of disease-characteristic features, should be excluded in advance. In this context, the image resolution of 224 × 224 pixels represents a critical threshold, as it is the maximum limit for input in many common neural network architectures [27,29]. On the other hand, neural network architectures allowing for higher resolution image input are available, but the processing of higher image resolutions increases the computing power demand. Limitations in the available computing power require specifications that limit the maximum image resolution intended for processing. This ensures the selection of a suitable deep neural network architecture that balances resource efficiency with the ability to handle task-appropriate image sizes. In order to provide scientific evidence and determine the requirements a neural network must fulfil, this project aimed to define the minimum resolution required for human experts to reliably classify ultrasound images of arteries commonly affected by GCA for the presence or absence of the disease.

METHODS

Study design

We designed a web-based exercise in which physicians experienced in GCA ultrasonography were asked to classify 250 ultrasound images for the presence or absence of GCA typical morphology. Forty-one physicians from 15 countries were invited by email to participate. To qualify as an expert, all participants must be board-certified rheumatologists with extensive experience in large-vessel vasculitis ultrasonography, defined as a minimum of 4 years interpreting GCA ultrasound images and prior assessment of at least 100 patients with suspected GCA throughout their careers. Additionally, they were members of the Large Vessel Vasculitis subgroup within the Outcome Measures in Rheumatology (OMERACT) Ultrasound subgroup. The study followed the principles of the Declaration of Helsinki and the Guidelines of Good Clinical Practice and received ethical approval from the local ethics committee (Institutional Review Board number #101/22). Patients and the public were not actively involved in the design and conduct of this study.

Vascular ultrasound image source and selection

CJB selected 50 ultrasound images from an image collection provided by 5 international experts in GCA ultrasonography (CM, CP, MM, VSS, and WAS). The selection included 10 images of each of the following vessels: (1) superficial common temporal arteries, (2) their frontal branch, (3) their parietal branch (all in transverse view), (4) axillary arteries in transverse view, and (5) axillary arteries in longitudinal view. All ultrasound

images were obtained in B-mode. The sample included 6 images from patients with acute GCA and 4 images from healthy individuals for each vessel, except for the axillary artery in longitudinal view, which had 5 images from patients with acute GCA and 5 images from healthy individuals. The images were obtained from a total of 50 patients, of which 29 had GCA and 21 had no evidence of GCA.

Each image was derived from an individual patient or a healthy subject. Images were obtained from different ultrasound machine brands (Esaote, GE, and Philips) using 3 to 12 (Philips EPIQ), 4 to 12 (GE LOGIQ e), 6 to 15 (GE LOGIQ S8), 5 to 18 (Philips EPIQ), 6 to 18 (Esaote MyLab 8), 8 to 18 (GE LOGIQ E9), and 6 to 24 MHz (GE LOGIQ E10) linear transducers for the investigation of axillary arteries and 5 to 18 (Philips EPIQ), 8 to 18 (GE LOGIQ S8 and GE LOGIQ E9), and 6 to 24 MHz (GE LOGIQ E10) hockey stick probes for the investigation of cranial arteries. Image acquisition at each site was performed according to a previously published scanning protocol [14]. Intima-media thickness (IMT) measurements were available for all images. All GCA patients had a diagnosis confirmed by a board-certified rheumatologist and met either the extension of the 2016 American College of Rheumatology classification criteria for GCA [30] or the 2022 American College of Rheumatology/EULAR classification criteria for GCA [31] (depending on the date of diagnosis). Diagnosis was confirmed either by TAB or imaging, including ultrasound. None of the patients had a change in clinical diagnosis from GCA to a non-GCA diagnosis during the follow-up period.

Vascular ultrasound image processing

All ultrasound images were individually loaded into an image editing software (GNU Image Manipulation Program version 2.10.8) to apply the necessary image preparation for this study. IMT measurements were removed if present. From each ultrasound image, a square 512 × 512-pixel image section focusing on the appropriate artery was selected and cut out. This section was subsequently downsized (without interpolation) to all study-specific resolution variants, namely 32 × 32, 64 × 64, 128 × 128, and 224 × 224 pixels. Figure 1 reflects the visual perception of all 5 image resolution variants applied in the study. All 4 downsized variants, in addition to the initial 512 × 512-pixel variant, resulted in a total of 250 vascular ultrasound images representing 50 distinct vessel images, each at 5 different resolutions.

Conduct of the web-based classification exercise

The web-based image classification exercise was performed via Research Electronic Data Capture (REDCap, provided by Vanderbilt University [32]) version 13.2.5. It included all vascular ultrasound images without any information about the

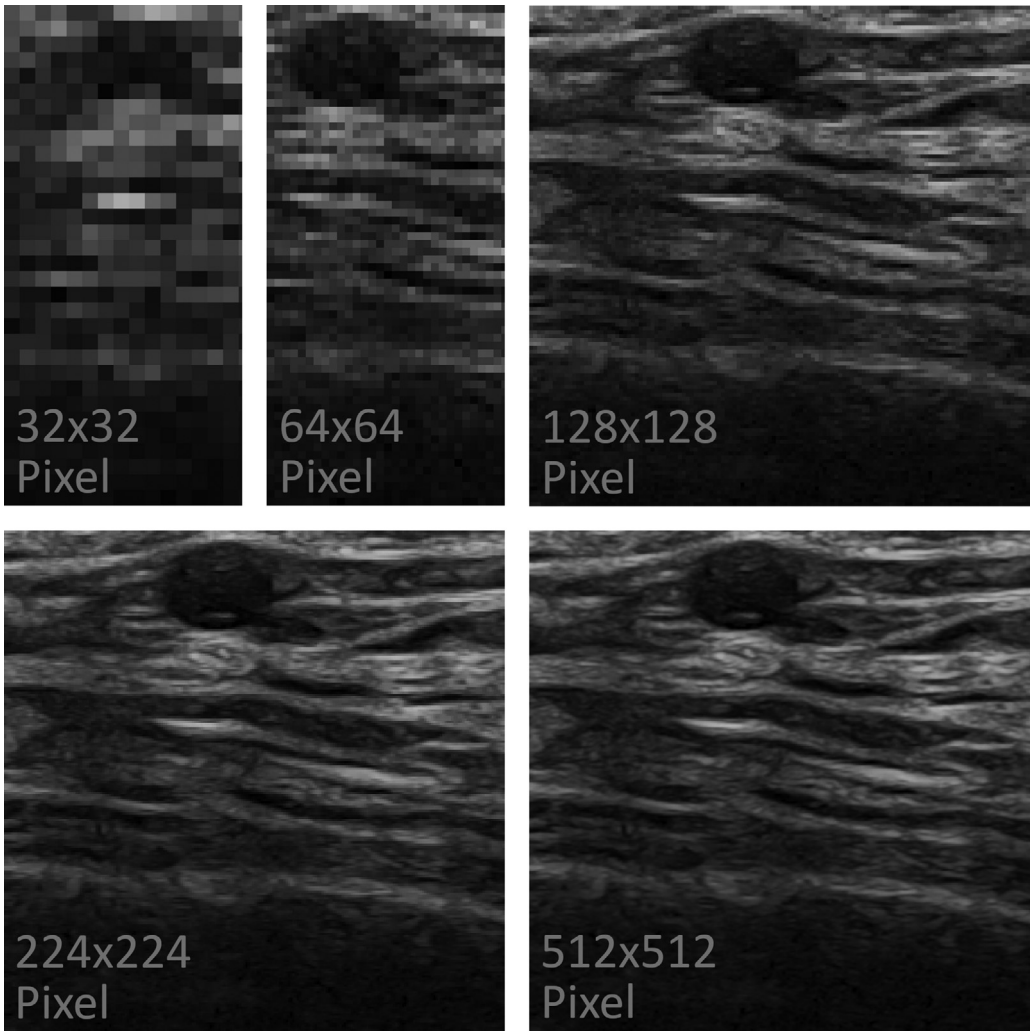

Figure 1. Comparison between the original square 512 × 512-pixel cut out from a native B-mode ultrasound image of the superficial common temporal artery in transversal view and its downsized study-specific resolution variants, namely 32 × 32, 64 × 64, 128 × 128, and 224 × 224 pixels.

corresponding IMT measurements, final ultrasound results, or clinical patient details. Intentionally, participants of the exercise were not told that they were evaluating identical images at different resolutions. To prevent image recall, images were displayed sequentially by artery and section, starting with the lowest resolution, with images presented in random order at each resolution level. During the classification exercise, each image was shown individually (1 per page), with each vascular ultrasound image representing a separate patient case (see Supplementary Fig S1). Participants were given 3 response options to the question, "I classify this ultrasound image as belonging to a …": (1) "GCA patient," (2) "Healthy individual," and (3) "Meaningful classification is not possible." Whenever the latter option was selected, a follow-up dialogue box appeared, prompting the participant to choose either "GCA patient" or "Healthy individual" in response to the question, "If only one of the above-mentioned answers was accepted, I would pick…" This approach to gathering 'forced classifications' aimed at a deeper understanding and recognition of patterns in the participants' decision-making process. Personal data regarding professional experience were also collected from all participants.

Statistical analysis

Statistical analyses were conducted using SPSS Statistics (version 26.0.0.0; IBM Corporation) and R (version 4.3.0; R Foundation for Statistical Computing) [33]. Descriptive statistics and exploratory data analysis were used. For metric parameters, mean, SD, median (in the case of the monthly average image classification figures, which contained individual outliers), and ranges were calculated. Categorical data were summarised by absolute and relative frequencies. Further analysis was performed to determine which change in image resolution is linked to a significant effect on correct image classification using logistic mixed-effects models. An increased chance of correct classification, indicated by an estimated odds ratio (OR) larger than 1, is interpreted as an improvement in classification performance. An estimated OR smaller than 1 is interpreted as a deterioration in image classification performance. To account for repeated measurements per rater and image, these were included as random intercept terms. Further factors impacting the classification decision, such as image resolution, working experience, and whether a study participant had provided study images, were investigated and, therefore, included as fixed effects. The image resolution and arteries were included as categorical independent variables. When the analyses were adjusted for the number of years experts had already been reading GCA ultrasound images or the number of patients that experts estimated to have seen, these were included as metric independent variables. Sensitivity and specificity were calculated on the basis of correct and incorrect classification numbers. In addition to that, 95% CIs were calculated. Due to a technical error in REDCap, detected only after study completion, participants could bypass the 'forced classification' within the follow-up question after the initial response had indicated an unclassifiable image. This affected all participants equally. Missing classifications from this issue were excluded from the analysis. The threshold for statistical significance was set at $p = .05$.

RESULTS

Study participant characteristics and expertise

Out of 41 international experts in GCA ultrasonography invited to participate in the web-based exercise, 31 responded, resulting in a response rate of 75.6%. The cohort comprised 5 board-certified rheumatologists from Denmark, 4 from the United States of America, 4 from Germany, 3 from Italy, 3 from Austria, 2 from the United Kingdom, 2 from the Netherlands, and 1 each from Bulgaria, Norway, Poland, Portugal, Slovenia, Spain, Switzerland, and Turkey. Study participants had an average of 21.2 years of medical experience, ranging from 9 to 40 years. They had been interpreting GCA ultrasound images for an average of 10.9 years, with experience ranging from 4 to 30 years. Participants reported evaluating a median of 16.0 (mean, 70.1; range, 2-500) images from GCA patients per month.

Image classification results

Overall, 7750 classification decisions were obtained (31 participants conducting a total of 310 decisions per artery, view and resolution combined).

Overall, the frequency of participants selecting the response option 'meaningful classification is not possible' decreased with increasing image resolution (constantly with every sequential stage of raised image resolution) from 90.5% (at the image resolution stage of 32 × 32 pixels) to 25.9% (at 512 × 512 pixels). Figure 2 illustrates how frequently the response option was selected during vascular ultrasound image classification, depending on the respective artery (and view) and image resolution. It was selected least frequently for images of the axillary artery in longitudinal view (19.0%), the axillary artery in transverse view (22.3%), and the temporal artery in transverse view (26.1%) at the 512 × 512-pixel resolution.

When experts initially selected 'meaningful classification is not possible,' they were subsequently asked to make a forced decision on whether the ultrasound image belonged to a GCA patient or a healthy individual (referred to as 'forced classification'). Table 1 presents detailed results of 'confident classification' provided in the first instance, as well as the 'forced classification' outcomes for all arteries, views, and image resolutions. Generally, increasing image resolution from 32 × 32 to 224 × 224 pixels led to a higher number and percentage of correct classifications across all arteries and views. This improvement was consistent whether considering only correct confident classifications (32 × 32 pixels: 4.8%; 64 × 64 pixels: 13.8%; 128 × 128 pixels: 37.7%; 224 × 224 pixels: 57.6%) or both confident and forced classifications (32 × 32 pixels: 37.8%; 64 × 64 pixels: 54.8%; 128 × 128 pixels: 68.6%; 224 × 224 pixels: 74.4%). No relevant increment was observed in classification results once image resolution increased further from 224 × 224 pixels to 512 × 512 pixels (overall correct confident classification at 512 × 512 pixels: 61.1%; overall correct confident and forced classification at 512 × 512 pixels: 75.3%).

A detailed view showed that the highest percentage of correct classifications was achieved in ultrasound images of the axillary artery in longitudinal view (total percentage of correct classifications at an image resolution of 512 × 512 pixels: 83.9%). Images of the axillary artery in transverse view yielded the lowest percentage of correct classifications at any image resolution stage compared with other combinations of arteries and views.

Further analysis of the complete dataset across all arteries and views revealed that any increase in image resolution significantly improved classification performance compared with the reference category of 32 × 32-pixel images. Specifically, image resolutions of 64 × 64 pixels (OR, 2.19; 95% CI, 1.84-2.61; $p < .001$), 128 × 128 pixels (OR, 3.49; 95% CI, 2.91-4.19; $p < .001$),

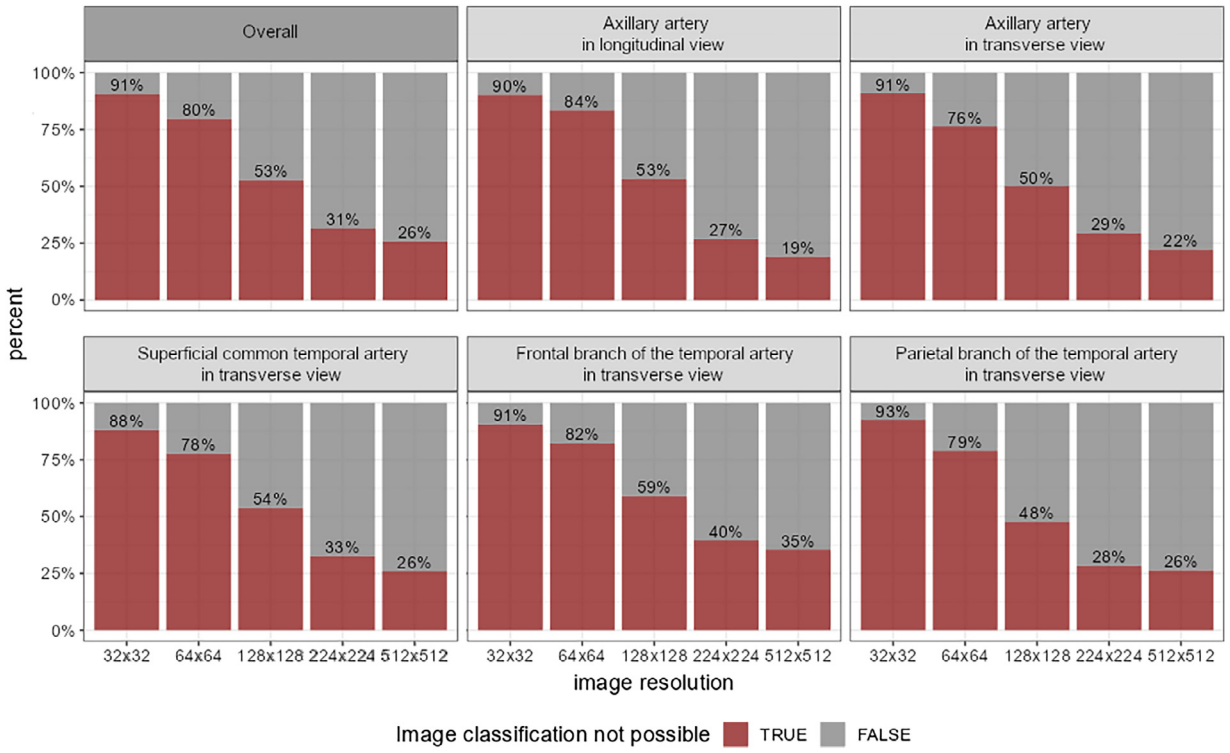

Figure 2. Frequency of the response option 'Meaningful classification is not possible' being selected during vascular ultrasound image classification, depending on the respective artery (and view) and image resolution. For all arteries, the frequency of this response option being selected decreased with increasing image resolution (consistent with every sequential stage of increased image resolution).

224 × 224 pixels (OR, 4.11; 95% CI, 3.42-4.94; $p < .001$), and 512 × 512 pixels (OR, 3.90; 95% CI, 3.25-4.69; $p < .001$) were all associated with significant improvements in image classification performance. In comparison with 128 × 128-pixel images as the reference category, increasing the image resolution further improved classification performance numerically, although the improvement did not reach statistical significance (224 × 224 pixels: OR, 1.18; 95% CI, 0.97-1.43; $p = .094$; 512 × 512 pixels: OR, 1.12; 95% CI, 0.93-1.35; $p = .248$). A subanalysis selectively considering images of the axillary artery in longitudinal view or the temporal artery in transverse view did not reveal any relevant differences in the overall trend compared with the main analysis.

Heatmap plots illustrating the frequency with which each individual image included in this web-based exercise was classified correctly at a certain image resolution level are enclosed in Supplementary Figure S2.

Sensitivity and specificity

The sensitivity and specificity of classifying vascular ultrasound images for the presence or absence of GCA indicative abnormalities based on single static B-mode images were assessed for any vessel/view and image resolution. Classification of 512 × 512-pixel longitudinal view images of the axillary artery achieved the highest specificity (specificity: 0.948, sensitivity: 0.734), while the lowest specificity was observed in 64 × 64-pixel transverse view images of the axillary artery (specificity: 0.596). Classification of 512 × 512-pixel transverse view images of the temporal artery's frontal branch achieved the highest sensitivity (sensitivity: 0.851, specificity: 0.793), while the lowest sensitivity was observed in 32 × 32-pixel transverse view images of the parietal branch of the temporal artery (sensitivity: 0.153). In general, sensitivity and specificity metrics constantly improved with rising image resolution between 32 × 32 and 128 × 128 pixels. In further increasing the image resolution beyond 128 × 128 pixels, sensitivity and specificity metrics continued to rise or remained constant, depending on the considered artery and view. Detailed data are listed in Table 2.

Factors impacting the classification decision

A logistic mixed-effects model, which was performed in order to detect influential factors in classification decision-making and potential confounders (study participants' contribution to study image provision, image resolution, study participants' level of experience in GCA image interpretation as quantified by temporal duration, and quantity of scans interpreted throughout their career), identified image resolution as the only significant determining factor. A lower image resolution had a higher chance that the image was marked as 'meaningful classification is not possible.' Compared with a resolution of 512 × 512 pixels, the chance of receiving the label 'Meaningful classification is not possible' (1: yes, 0: no) was increased by a factor of 1.43 ($p < .001$) for images of size 224 × 224 pixels, a factor of 5.05 ($p < .001$) for images of size 128 × 128 pixels, a factor of 40.97 ($p < .001$) for images of size 64 × 64 pixels, and a factor of 198.84 ($p < .001$) for images of size 32 × 32 pixels. Likewise, compared with a resolution of 512 × 512 pixels, lower image resolutions led to significantly lower rates of correct image classification (eg, for an image size of 32 × 32 pixels: OR, 0.25; $p < .001$; for an image size of 64 × 64 pixels: OR, 0.56; $p < .001$). The number of years experts had already been reading GCA ultrasound images had no significant effect on the selection of the response category 'Meaningful classification is not possible' (OR, 1.02;

Table 1
Image classification results across all arteries, views, and image resolutions (in pixels)

		Confident classification			Forced classification						
Location	Pixel	Correct	Incorrect	Not possible ↳	Correct	Incorrect	Not answered	% confident correct	% total correct*	% confident incorrect	% total incorrect**
Axillary artery - Longitudinal view	**32x32**	18	12	280	92	99	89	5.81	35.48	3.87	35.81
	64x64	38	13	259	146	51	62	12.26	59.35	4.19	20.65
	128x128	124	21	165	112	26	27	40.00	76.13	6.77	15.16
	224x224	201	26	83	49	27	7	64.84	80.65	8.39	17.10
	512x512	227	24	59	33	25	1	73.23	83.87	7.74	15.81
Axillary artery - Transverse view	**32x32**	12	16	282	98	106	78	3.87	35.48	5.16	39.35
	64x64	49	24	237	97	78	62	15.81	47.10	7.74	32.90
	128x128	113	42	155	70	42	43	36.45	59.03	13.55	27.10
	224x224	172	47	91	35	28	28	55.48	66.77	15.16	24.19
	512x512	176	65	69	29	19	21	56.77	66.13	20.97	27.10
Superficial common temporal artery - Transverse view	**32x32**	19	18	273	105	85	83	6.13	40.00	5.81	33.23
	64x64	42	27	241	117	64	60	13.55	51.29	8.71	29.35
	128x128	115	28	167	87	41	39	37.10	65.16	9.03	22.26
	224x224	166	43	101	52	18	31	53.55	70.32	13.87	19.68
	512x512	180	49	81	43	16	22	58.06	71.94	15.81	20.97
Frontal branch of the temporal artery - Transverse view	**32x32**	14	15	281	112	92	77	4.52	40.65	4.84	34.52
	64x64	38	17	255	142	39	74	12.26	58.06	5.48	18.06
	128x128	99	28	183	128	20	35	31.94	73.23	9.03	15.48
	224x224	159	28	123	70	23	30	51.29	73.87	9.03	16.45
	512x512	168	32	110	68	17	25	54.19	76.13	10.32	15.81
Parietal branch of the temporal artery - Transverse view	**32x32**	11	12	287	105	112	70	3.55	37.42	3.87	40.00
	64x64	47	18	245	134	56	55	15.16	58.39	5.81	23.87
	128x128	133	29	148	82	24	42	42.90	69.35	9.35	17.10
	224x224	194	28	88	55	8	25	62.58	80.32	9.03	11.61
	512x512	196	32	82	47	11	24	63.23	78.39	10.32	13.87

During the image classification exercise, experts first chose 1 of 3 options to answer the question, "I classify this ultrasound image as belonging to a . . .": (1) "GCA patient," (2) "Healthy individual," or (3) "Meaningful classification is not possible." This initial decision is termed "Confident classification" (results in the first 3 columns). If option (3) was selected, a follow-up dialogue prompted a forced choice between "GCA patient" and "Healthy individual" (termed 'Forced classification,' results in the next 3 columns). Percentage figures can be found in the 4 columns on the right. In total, 310 classifications were submitted for each artery, view, and image resolution (10 images classified by 31 experts).
[a]Percent total correct: the number of correct confident classifications plus the number of correct forced classifications, divided by the total number of classifications (n = 310).
[b]Percent total incorrect: the number of incorrect confident classifications plus the number of incorrect forced classifications, divided by the total number of classifications (n = 310).

$p = .725$). Neither did the number of patients that experts estimated to have seen and evaluated for suspected GCA throughout their career (OR, 1.00; $p = .422$). The presented statistical data were derived from a model adjusted for differences across artery locations and views.

DISCUSSION

In this first and international study exploring the minimum image resolution mandatory for reliable human expert classification of vascular ultrasound images in GCA and healthy subjects, we observed ascending classification performance with increasing image resolution up to an image resolution of 224 × 224 pixels, where decision confidence and image classification performance plateaued without further significant gains despite a continual increase in image resolution.

In fact, an in-depth analysis of the classification exercise performed in this study by human experts revealed that, compared with images of 128 × 128 pixels set as the reference category, higher image resolutions still showed further numerical

Table 2
Sensitivity and specificity of vascular ultrasound image classification by human experts at various image resolutions, arteries, and views

Artery	Metric	Image resolution (pixels)				
		32 × 32	64 × 64	128 × 128	224 × 224	512 × 512
Overall	Sensitivity	0.299	0.585	0.755	0.767	0.761
	Specificity	0.814	0.832	0.814	0.862	0.856
Axillary artery—longitudinal view	Sensitivity	0.328	0.549	0.727	0.733	0.734
	Specificity	0.719	0.929	0.943	0.915	0.948
Axillary artery—transverse view	Sensitivity	0.350	0.584	0.707	0.702	0.678
	Specificity	0.663	0.596	0.65	0.784	0.757
Superficial common temporal artery—transverse view	Sensitivity	0.346	0.549	0.759	0.734	0.709
	Specificity	0.846	0.773	0.724	0.855	0.871
Frontal branch[a]—transverse view	Sensitivity	0.329	0.690	0.837	0.834	0.851
	Specificity	0.860	0.872	0.807	0.793	0.793
Parietal branch[a]—transverse view	Sensitivity	0.153	0.555	0.738	0.829	0.830
	Specificity	0.979	0.950	0.898	0.939	0.878

[a] Branch of the temporal artery.

improvement in classification performance. However, classification performance improvement with increasing image resolution largely plateaued at 224 × 224 pixels, in line with sensitivity and specificity metrics, which also accentuated a 'sweet spot' at 224 × 224 pixels. In a combined conservative consideration of these results, an image resolution of 224 × 224 pixels crystallised as the optimum between preserved information content and data size efficiency, thereby defining the minimum requirement for image resolution a neural network architecture in this scenario of application will be supposed to handle. These findings resonate with the applied image resolution in other application scenarios of AI-driven medical imaging classifications [34,35] in general, but more specifically, vessel ultrasound image classification within the scope of disorders other than GCA [36,37]. Particularly noteworthy is a study conducted by Li et al [37], which similarly focused on the detection of disease-specific vascular wall changes—in this case, the automatic detection of atherosclerotic plaques and calcification from intravascular ultrasound images. Despite contextual differences, parallels to our study's conclusions can be drawn from the fact that Li et al [37] also successfully trained their neural network with images at a resolution of 224 × 224 pixels. Our study provides evidence that adequate GCA ultrasound image classification by human experts does not necessarily require the highest resolution level of 512 × 512 pixels, but can be appropriately achieved at a resolution level of 224 × 224 pixels. This finding broadens the range of neural network architectures suitable for AI development, including the widely chosen and resource-efficient network architectures such as ResNet [27] or DenseNet [29], which are limited to a maximum default image input size of 224 × 224 pixels.

Moreover, the reported results on human expert image classification performance serve as an essential benchmark for the classification performance of the projected neural network, which aims to match or exceed human expert classification performance, as achieved in other medical fields before [35]. The data presented in this study are representative, particularly considering that experts were only provided with 1 single static B-mode image per patient without any additional IMT measurement, halo, compression sign, insight into other anatomical segments, or clinical information. While participants in this study classified each image individually, it is important to note that there are typically 8 or more images available per patient, which may lead to higher sensitivity and lower specificity on a patient level when combined in clinical practice. Also, sensitivity and specificity results, combined with heatmap visualisation (Supplementary Fig S2) and data from both confident and forced classifications, indicate that participants tended to classify an image as belonging to a GCA patient only when they were relatively confident. Among all cases in which the initial response option had been 'meaningful classification is not possible,' subsequent forced classifications found more than twice as many of these images to be attributed to GCA patients vs healthy individuals. Thus, images ultimately classified as belonging to GCA patients were clearly overrepresented within the category of 'meaningful classification is not possible' initial responses. This superordinate dynamic likely contributed to missed GCA classifications, explaining the persistent rate of misclassifications even at higher image resolutions. At the same time, this caused assessment specificity to remain consistently high across all resolution stages. Despite all these factors, the image classification performance yielded remarkable sensitivity and specificity results. Our reported sensitivity of 0.833 and specificity of 0.915 for 224 × 224-pixel longitudinal view images of the axillary artery, as well as 0.734 and 0.855, respectively, for 224 × 224-pixel transverse view images of the superficial common temporal artery, align with data from a systematic review and meta-analysis investigating the diagnostic performance of temporal artery ultrasound (considering full resolution images) for the diagnosis of GCA [38]. This meta-analysis, based on 11 studies with available data, reported a sensitivity of 0.78 and a specificity of 0.79 for detecting any sono-morphologic abnormalities (hypoechoic halo, stenosis, and/or occlusion) in GCA ultrasound. Likewise, this study's results are in line with the results of the OMERACT Patient-based Reliability Exercise [14] that yielded an interreader reliability of around 0.8 (light κ, 0.76-0.86) for the overall diagnosis of GCA.

Limitations included the natural restrictions in expert availability to participate in this exercise. Indeed, 5 experts participated in this study who had previously granted access to their image libraries, out of which a fraction of images was randomly selected by an independent individual (CJB) not involved as a study participant. In weighing whether these study participants may have contributed to a bias in the results, we performed sensitivity analyses for all reported metrics, which did not lead to a significant change in results after the exclusion of these participants. Image selection may have been subject to selection bias and holds the potential to have impaired representativeness. Furthermore, we decided

not to actively include or exclude ultrasound images containing aspects of atherosclerosis, where an OMERACT ultrasound definition is available and validated [15]. Instead, our dataset represents a random sampling from real-world clinical cases, not stratified based on comorbidities. While in fact, fibromuscular dysplasia or many other vasculopathies are rarely encountered in temporal and axillary arteries, and atherosclerosis is also uncommon in temporal arteries, atherosclerotic changes can occur in the axillary arteries, though they are typically distinguishable by ultrasound based on their characteristic morphology [15]. Nonetheless, future research should explore whether higher image resolution is needed to differentiate GCA from these specific mimics, particularly in borderline cases where classification might be more challenging. Intentionally and with the operating principle of the projected AI-based GCA ultrasound image classification assistant in mind (see Supplementary Material), this study made use of a single static B-mode image per patient case without any additional IMT measurement, halo, compression sign, or clinical information. This represents a striking difference in the way human experts are used to approach a classification decision in clinical practice when performing GCA ultrasound in a dynamic manner, with appraisal of multiple anatomical segments. We regard this as the primary reason for the overall high rate of initially 'non-classifiable' images. An intrarater exercise could also have been conducted, but it was felt to be beyond the scope of this project. A technical error in REDCap allowed the omission of forced classifications, resulting in missing values within the dataset. While potential bias cannot be entirely excluded, removing these missing classifications was deemed the most appropriate strategy to minimise bias. For transparency, Table 1 presents a detailed breakdown of classification results across all arteries, views, and image resolutions for both confident and forced classifications.

In conclusion, this international online study evaluated the minimum image resolution mandatory for reliable human expert classification of vascular ultrasound images in GCA and healthy subjects and found that 224 × 224-pixel images provide the optimum between preserved information content and data size efficiency. This opens up a broad variety of applicable deep neural network architectures for the development of an AI-based assistant.

Future directions

Building on the results of the present study as the technical foundation, the realisation of an AI-based GCA ultrasound image classification assistant, as ultimately envisioned, follows a modularly structured project roadmap, specific intermediate milestones, and developmental steps that can be briefly outlined as follows:

1. Training and validating a neural network model utilising a task-appropriate dataset.
2. Expert-led clinical validation to prove reliability.
3. Staged rollout into clinical routine care.

While the primary developed neural network focuses on vessel morphology and pathological IMT in B-mode ultrasound images, it will subsequently be accompanied by 2 additional complementary neural networks that are to be developed for the evaluation of halo and compression signs. Each of these models will independently undergo the same steps of (1) dataset development, training, and validation, as well as (2) expert-led clinical evaluation before undergoing (3) a staged rollout into routine care. To date, a 3800-ultrasound image library has already been provided for deep neural network training. Once development and clinical validation of the AI model have been completed, a publicly accessible website hosting the AI-based assistant that facilitates the classification of uploaded ultrasound images and helps to diagnose GCA early is envisioned. This approach holds great potential for the rapid and accurate diagnosis of GCA, including in resource-disadvantaged regions, a factor that could critically impact individuals by allowing diagnosis before ischaemic complications occur.

Competing interests

All authors declare they have no competing interests.

Acknowledgements

SLM is supported in part by the NIHR Leeds Biomedical Research Centre (NIHR203331). The views expressed in this article are those of the authors and not necessarily those of the NIHR, the NIHR Leeds Biomedical Research Centre, the National Health Service, or the UK Department of Health and Social Care.

Contributors

C-JB: conceptualisation, methodology, validation, formal analysis, investigation, resources, data curation, writing (original draft), writing (review and editing), visualisation, supervision, and project administration. SC: methodology, software, validation, investigation, resources, data curation, writing (review and editing), and funding acquisition. WAS, MM, CP, and CBM: investigation, resources, and writing (review and editing) C Dejaco, MJ Koster, MJ Kohler, SM, WAS, PK, MM, CP, CBM, C Duftner, EdM, AH, AI, LT, UMD, BDN, AJ, LS, KKK, RK, TD, SLM, KT, KSMvdG, DB, PB, AT, MA, TAK, AD, UF, NI, SMP, SA: investigation and writing (review and editing). CB: formal analysis, resources, writing (original draft), writing (review and editing), and visualisation. VSS: methodology, investigation, resources, writing (original draft), writing (review and editing), supervision, and internal funding acquisition.

Funding

This study received no specific funding.

Patient consent for publication

Not applicable.

Ethics approval

The study received ethical approval from the local ethics committee (Institutional Review Board number #101/22).

Provenance and peer review

Not commissioned; externally peer reviewed.

Data availability statement

Any dataset parts generated and analysed for this study that are not already included in this article are available upon

reasonable request. Further inquiries can be directed to the corresponding author.

Supplementary materials

Supplementary material associated with this article can be found in the online version at doi:10.1016/j.ard.2025.05.010.

Orcid

Claus-Juergen Bauer: http://orcid.org/0000-0003-3152-6550
Matthew J. Koster: http://orcid.org/0000-0002-2895-6755
Minna J. Kohler: http://orcid.org/0000-0001-6450-7546
Wolfgang A. Schmidt: http://orcid.org/0000-0001-7831-8738
Chetan B. Mukhtyar: http://orcid.org/0000-0002-9771-6667
Marcin Milchert: http://orcid.org/0000-0002-0943-8768
Alojzija Hocevar: http://orcid.org/0000-0002-7361-6549
Luca Seitz: http://orcid.org/0000-0002-5051-1445
Sarah Louise Mackie: http://orcid.org/0000-0003-2483-5873
Dennis Boumans: http://orcid.org/0000-0002-2150-6065
Simon M. Petzinna: http://orcid.org/0000-0002-4686-1143
Charlotte Behning: http://orcid.org/0000-0002-9310-3804

REFERENCES

[1] Aiello PD, Trautmann JC, McPhee TJ, Kunselman AR, Hunder GG. Visual prognosis in giant cell arteritis. Ophthalmology 1993;100:550–5.
[2] Salvarani C, Cimino L, Macchioni P, Consonni D, Cantini F, Bajocchi G, et al. Risk factors for visual loss in an Italian population-based cohort of patients with giant cell arteritis. Arthritis Rheum 2005;53:293–7.
[3] Pariente A, Guédon A, Alamowitch S, Thietart S, Carrat F, Delorme S, et al. Ischemic stroke in giant-cell arteritis: French retrospective study. J Autoimmun 2019;99:48–51.
[4] Caselli RJ, Hunder GG. Neurologic complications of giant cell (temporal) arteritis. Semin Neurol 1994;14:349–53.
[5] Gonzalez-Gay MA, Vazquez-Rodriguez TR, Gomez-Acebo I, Pego-Reigosa R, Lopez-Diaz MJ, Vazquez-Triñanes MC, et al. Strokes at time of disease diagnosis in a series of 287 patients with biopsy-proven giant cell arteritis. Medicine (Baltimore) 2009;88:227–35.
[6] Gonzalez-Gay MA, Garcia-Porrua C, Piñeiro A, Pego-Reigosa R, Llorca J, Hunder GG. Aortic aneurysm and dissection in patients with biopsy-proven giant cell arteritis from northwestern Spain: a population-based study. Medicine (Baltimore) 2004;83:335–41.
[7] Hellmich B, Agueda A, Monti S, Buttgereit F, de Boysson H, Brouwer E, et al. 2018 Update of the EULAR recommendations for the management of large vessel vasculitis. Ann Rheum Dis 2020;79:19–30.
[8] Luqmani R, Lee E, Singh S, Gillett M, Schmidt WA, Bradburn M, et al. The role of ultrasound compared to biopsy of temporal arteries in the diagnosis and treatment of giant cell arteritis (TABUL): a diagnostic accuracy and cost-effectiveness study. Health Technol Assess 2016;20:1–238.
[9] Schmidt WA. Ultrasound in the diagnosis and management of giant cell arteritis. Rheumatology (Oxford) 2018;57:ii22–31.
[10] Karakostas P, Dejaco C, Behning C, Recker F, Schäfer VS. Point-of-care ultrasound enables diagnosis of giant cell arteritis with a modern innovative handheld probe. Rheumatology (Oxford) 2021;60:4434–6.
[11] Schmidt WA, Kraft HE, Vorpahl K, Völker L, Gromnica-Ihle EJ. Color duplex ultrasonography in the diagnosis of temporal arteritis. N Engl J Med 1997;337:1336–42.
[12] Aschwanden M, Imfeld S, Staub D, Baldi T, Walker UA, Berger CT, et al. The ultrasound compression sign to diagnose temporal giant cell arteritis shows an excellent interobserver agreement. Clin Exp Rheumatol 2015;33 S-113-5.
[13] De Miguel E, Castillo C, Rodríguez A, De Agustín JJ. Working Group Ultrasound Giant Cell Arteritis. Learning and reliability of colour Doppler ultrasound in giant cell arteritis. Clin Exp Rheumatol 2009;27:S53–8.
[14] Schäfer VS, Chrysidis S, Dejaco C, Duftner C, Iagnocco A, Bruyn GA, et al. Assessing vasculitis in giant cell arteritis by ultrasound: results of OMERACT Patient-based Reliability Exercises. J Rheumatol 2018;45:1289–95.
[15] Chrysidis S, Duftner C, Dejaco C, Schäfer VS, Ramiro S, Carrara G, et al. Definitions and reliability assessment of elementary ultrasound lesions in giant cell arteritis: a study from the OMERACT Large Vessel Vasculitis Ultrasound Working Group. RMD Open 2018;4:e000598.
[16] Chrysidis S, Terslev L, Christensen R, Fredberg U, Larsen K, Lorenzen T, et al. Vascular ultrasound for the diagnosis of giant cell arteritis: a reliability and agreement study based on a standardised training programme. RMD Open 2020;6:e001337.
[17] Dejaco C, Ramiro S, Bond M, Bosch P, Ponte C, Mackie SL, et al. EULAR recommendations for the use of imaging in large vessel vasculitis in clinical practice: 2023 update. Ann Rheum Dis 2024;83:741–51.
[18] Coath FL, Bukhari M, Ducker G, Griffiths B, Hamdulay S, Hingorani M, et al. Quality standards for the care of people with giant cell arteritis in secondary care. Rheumatology (Oxford) 2023;62:3075–83.
[19] Terslev L, Hammer HB, Torp-Pedersen S, Szkudlarek M, Iagnocco A, D'Agostino MA, et al. EFSUMB minimum training requirements for rheumatologists performing musculoskeletal ultrasound. Ultraschall Med 2013;34:475–7.
[20] Muratore F, Pipitone N, Salvarani C, Schmidt WA. Imaging of vasculitis: state of the art. Best Pract Res Clin Rheumatol 2016;30:688–706.
[21] Chakraborty U, Banerjee A, Saha JK, Sarkar N, Chakraborty C. Artificial intelligence and the fourth industrial revolution. CRC Press; 2022.
[22] Amisha Malik P, Pathania M, Rathaur VK. Overview of artificial intelligence in medicine. J Family Med Prim Care 2019;8:2328–31.
[23] Irvin J, Rajpurkar P, Ko M, Yu Y, Ciurea-Ilcus S, Chute C, et al. Chexpert: a large chest radiograph dataset with uncertainty labels and expert comparison. In: Proceedings of the AAAI Conference on Artificial Intelligence. Honolulu, Hawaii, USA; Palo Alto (CA): AAAI Press; 2019. p. 590–7.
[24] Esteva A, Kuprel B, Novoa RA, Ko J, Swetter SM, Blau HM, et al. Dermatologist-level classification of skin cancer with deep neural networks. Nature 2017;542:115–8.
[25] McKinney SM, Sieniek M, Godbole V, Godwin J, Antropova N, Ashrafian H, et al. International evaluation of an AI system for breast cancer screening. Nature 2020;577:89–94.
[26] Andersen JKH, Pedersen JS, Laursen MS, Holtz K, Grauslund J, Savarimuthu TR, et al. Neural networks for automatic scoring of arthritis disease activity on ultrasound images. RMD Open 2019;5:e000891.
[27] Bressem KK, Vahldiek JL, Adams L, Niehues SM, Haibel H, Rodriguez VR, et al. Deep learning for detection of radiographic sacroiliitis: achieving expert-level performance. Arthritis Res Ther 2021;23:106.
[28] Alom MZ, Taha TM, Yakopcic C, Westberg S, Sidike P, Nasrin MS, et al. The history began from AlexNet: A comprehensive survey on deep learning approaches. arXiv:1803.01164 [Preprint]. 2018 [cited 2022 Dec 2]; [39 p.]. Available from: https://arxiv.org/abs/1803.01164.
[29] Riasatian A, Babaie M, Maleki D, Kalra S, Valipour M, Hemati S, et al. Fine-tuning and training of densenet for histopathology image representation using tcga diagnostic slides. Med Image Anal 2021;70:102032.
[30] Salehi-Abari I. 2016 ACR revised criteria for early diagnosis of giant cell (temporal) arteritis. Autoimmune Dis Ther Approaches 2016;3:1–4.
[31] Ponte C, Grayson PC, Robson JC, Suppiah R, Gribbons KB, Judge A, et al. 2022 American College of Rheumatology/EULAR classification criteria for giant cell arteritis. Arthritis Rheumatol 2022;74:1881–9.
[32] Harris PA, Taylor R, Thielke R, Payne J, Gonzalez N, Conde JG. Research Electronic Data Capture (REDCap)—a metadata-driven methodology and workflow process for providing translational research informatics support. J Biomed Inform 2009;42:377–81.
[33] R Core Team. R: a language and environment for statistical computing [Internet]. Vienna, Austria: R Foundation for Statistical Computing; 2023. [cited 2023 Apr 17]. Available from: http://www.R-project.org/.
[34] Sabottke CF, Spieler BM. The effect of image resolution on deep learning in radiography. Radiol Artif Intell 2020;2:e190015.
[35] Zunair H, Ben Hamza A. Melanoma detection using adversarial training and deep transfer learning. Phys Med Biol 2020;65:135005.
[36] Xie M, Li Y, Xue Y, Shafritz R, Rahimi SA, Ady JW, et al. Vessel lumen segmentation in internal carotid artery ultrasounds with deep convolutional neural networks. In: 2019 IEEE International Conference on Bioinformatics and Biomedicine (BIBM); 2019. p. San Diego, CA, USA2393–8.
[37] Li YC, Shen TY, Chen CC, Chang WT, Lee PY, Huang CJ. Automatic detection of atherosclerotic plaque and calcification from intravascular ultrasound images by using deep convolutional neural networks. IEEE Trans Ultrason Ferroelectr Freq Control 2021;68:1762–72.
[38] Rinagel M, Chatelus E, Jousse-Joulin S, Sibilia J, Gottenberg JE, Chasset F, et al. Diagnostic performance of temporal artery ultrasound for the diagnosis of giant cell arteritis: a systematic review and meta-analysis of the literature. Autoimmun Rev 2019;18:56–61.